Prediction of the effectiveness of rolling dynamic compaction using artificial neural networks and cone penetration test data

R. A. T. M. Ranasinghe，M. B. Jaksa，F. Pooya Nejad，Y. L. Kuo

(*School of Civil，Environmental and Mining Engineering，University of Adelaide，Adelaide* 5005，*Australia*)

Abstract：Rolling Dynamic Compaction (RDC)，which is a ground improvement technique involving non-circular modules drawn behind a tractor，has provided the construction industry with an improved ground compaction capability，especially with respect to a greater influence depth and a higher speed of compaction，resulting in increased productivity. However，to date，there is no reliable method to predict the effectiveness of RDC in a range of ground conditions. This paper presents a new and unique predictive tool developed by means of artificial neural networks (ANNs) that permits *a priori* prediction of density improvement resulting from a range of ground improvement projects that employed 4-sided RDC modules；commercially known as "impact rollers". The strong coefficient of correlation (i.e. $R>0.86$) and the parametric behavior achieved in this study indicate that the model is successful in providing reliable predictions of the effectiveness of RDC in various ground conditions.

Key words：soil mechanics；rolling dynamic compaction；artificial neural networks；cone penetration test；ground improvement

CLC number TU 43 **Document code** A **Article ID** 1000－6915(2019)01－0153－18

1 Introduction

Compaction is the method of densification of soil by means of mechanically applied energy. A rapid volume reduction takes place during the compaction process due to pore air expulsion，which results in particle rearrangement and sometimes crushing. A number of methods are widely used in ground compaction，such as vibration，impact，kneading and static pressure. These different types of compaction techniques are essentially subdivided into two categories；static and dynamic compaction. Static compaction is the application of a downward force on the ground surface by the self-weight of the equipment，such as circular rollers，which usually employ drums，pad foots and pneumatic multi-tires. Dynamic compaction methods，on the other hand，apply a kinetically-driven downward force，in addition to the equipment′s self-weight. Dynamic compaction makes use of heavy tamping，vibratory drums and plates，rammers，vibroflotation and rolling dynamic compaction[1].

Rolling dynamic compaction (RDC) has increasingly become popular over the past few decades in the global construction industry and provides an alternative to the traditional approaches of soil compaction[2]. RDC was originally developed by Aubrey Berrangé in South Africa in the late 1940s，but its value was not fully realized until the mid-1980s. It involves towing heavy (6－12 tonnes) non-circular modules (3-，4- and 5-sided)，which rotate about their corners and fall to impact the ground[3]. For instance，Figure 1 illustrates the 4-sided impact roller module，which is towed by a tractor. As the impact roller traverses the ground，the

Received date：2017－12－11；**Revised date**：2018－08－22
Corresponding author：R.A.T.M. Ranasinghe. E-mail：tara.ranasinghe@gmail.com
DOI：10.13722/j.cnki.jrme.2017.1586

module rotates about its corners due to friction，and a series of high amplitude blows are delivered to the ground at a relatively low frequency of 90 to 130 blows per minute[4]. Thus，the compactive effort is derived from the energy of the mass falling from a corner to the adjacent compacting face of the polygonal shaped mass. This results in deep compaction and a greater influence depth – more than 1 m beneath the ground surface and sometimes as deep as 3 m in some soils[5] – compared to the conventional static and vibratory compaction[6-8]，which generally influences depths less than 0.5 m below the ground. As a result，thicker lifts，in excess of 0.5 m can be employed as compared to traditional compaction lifts of approximately 0.15 m[3，9]. Furthermore，RDC is particularly efficient when employed in large and open sites，as it traverses the ground at speeds of 9－12 km/h compared to traditional vibratory roller，which travels at 4 km/h[2]. As a consequence，RDC has been applied：(1) to the in situ densification of existing fills，such as on brownfield sites，landfills，earth embankments and sub grade proof-rolling[10]；(2) in the agricultural sector[3]，mainly for the improvement of existing water storages，channels and embankments；(3) in the mining industry for the construction of tailing dams[9]，rock demolition in open cut mine waste tips，compaction of the capping over waste rocks[11]，compaction of bulk earthworks of mine spoil materials and to induce fracturing on surface layers in rock quarries in lieu of drilling and blasting[9].

Fig.1　Four-sided impact roller towed behind a tractor

To date a number of field and case studies have assessed the efficacy of RDC. As a result，RDC is often adopted based on experience from previous work undertaken in similar soils and site conditions. In most cases，in order to determine the optimal number of RDC passes to achieve the design specifications，a field trial is undertaken，where measurements of various soil characteristics are obtained before and after compaction.

This study aims to develop a robust predictive model to forecast the performance of RDC by means of the artificial intelligence (AI) technique known as artificial neural networks (ANNs). It is intended that the model will provide additional，*a priori* information to supplement field trials undertaken on site prior to ground improvement. Attention is focused on the 4-sided，8 tonne“impact roller”(BH－1300). ANN models have been developed based on the cone penetration test (CPT) data，which are collected from previous ground improvement projects in Australia that employed RDC. Design equations are developed based on model parameters，and a parametric study is carried out to assess the robustness of the model. It is important to note that no such predictive model exists for RDC，neither empirical，theoretical nor numerical.

2　Database and data analysis

The data used in this study have been obtained from the results of several field trials undertaken by Broons SA Hire，an Australian company marketing a range of ground improvement technologies，including RDC. The database is comprised of in situ strength data in the form of cone penetration test (CPT) results with respect to the number of roller passes. CPT measurements provide continuous soil profiles that express variations of soil strength in terms of cone tip resistance (q_c) and sleeve friction (f_s). The CPT is often used as a profiling tool employing the friction ratio，which is the ratio，expressed as a percentage，of sleeve friction to cone tip resistance，measured at the same depth. The literature contains several soil classification charts based on the friction ratio as a function of cone tip resistance[12].

The CPT[13] has been widely used for monitoring and evaluating the effectiveness of deep compaction methods because of the continuous，reliable and repeatable nature of the measurements[14]. D. L. Avalle

and J. P. Carter[5] investigated the depth of influence of RDC in sandy soils using CPT profiles of prior to and after impact rolling，where a noticeable improvement was evident between depths of approximately 0.5 – 3 m below the ground surface. Moreover，research by D. B. Kelly[15] presented the results from CPTs where a significant depth of influence of RDC was evident to depths of 4 m in natural sand and un-compacted/ un-controlled variable clay fill，and in the reclaimed sand deposit to the depths of 5 m below the surface. Another recent case study conducted by B. T. Scott and M. B. Jaksa[16] reported on the verification of RDC，both vertically and laterally，in a sand fill having quantified the differences in cone tip resistance between a series of closely-spaced CPT locations.

The database used for ANN modelling is summarized in Table 1 and the data were acquired from Broons′ records of previous projects. Figure 2 shows typical plots of cone tip resistance and sleeve friction measurements which are obtained at essentially the same location prior to (0 passes) and after (10 passes and 20 passes) of RDC. As can be seen，there is a noticeable variation in cone tip resistance and sleeve friction measurements with respect to the number of roller passes. The differences between these individual measurements quantify the variation of soil strength and density，as well as a minor degree of spatial variation，resulting from RDC at the test location.

However，the CPT measurements are influenced by large，hard particles present in the compaction material and may not be representative of the subsurface condition，particularly at sites with uncontrolled fill. As a result，some localized peaks are visible in the CPT measurements，predominantly in the cone tip resistance measurements. As such，the CPT measurements are often accompanied by data anomalies that require a further processing and interpretation prior to their use in ANN modeling. However，in the data pre-processing，these anomalies are filtered from the dataset，otherwise the derived ANN models will be vulnerable to learning these random and unrepresentative irregularities. This is achieved by scrutinizing the individual CPT plots and manually removing the unreliable measurements，based on experience of the CPT operation and procedure，the local geological conditions and past experience with similar project sites. For instance，during the data preprocess the CPT plots were scrutinized to identify the sudden variations of CPT measurements. Because，the CPT soundings are often influenced by large，hard particles present in the compaction material and the data may not be representative of the subsurface condition，particularly at sites with uncontrolled fill. As a result，some localized peaks are visible in the CPT measurements，predominantly in the cone tip resistance measurements. In that case，a number of CPT plots from adjacent CPT soundings are superimposed to highlight the localized peaks present due to the spatial variability of the compacted material. These measurements were removed from the data set during the preprocessing stage. However，it should be noted that the dataset still contains several measurements of q_{ci} and q_{cf} that can be considered as higher than usual. In such circumstances，the authors had no compelling reason to consider them as unrealistic，rather considering them to be related to a very firm soil.

In this study，CPT measurements are considered for the depth range of 0.1 m to 4 m. It is well established in RDC，that a significant reduction in the soil strength in the upper 0.1 m is always evident due

Table 1 Summary of CPT plots

No	Project name	Max. depth/m	No. of CPT locations	Soil type	No. of roller passes at the time of test
1	Port Botany	9.8	64	Sandy/silty sandy fill overlying marine deposits of sand and peaty clay deposits	0，10，20，30，40
2	Potts Hill	8.8	19	Shale fill overlying residual soil and sandstone bedrock	0，10，20，30，40
3	Outer Harbor	3.8	8	Uncontrolled fill overlying St. Kilda formation soils	0，24
4	Banksmeadow	6.2	3	Silty sandy filling overlying natural sands	0，5，20
5	Cairns	4.9	9	Uncontrolled fill underlain by silty clay/clayey silt/sandy silt	0，20，30，40

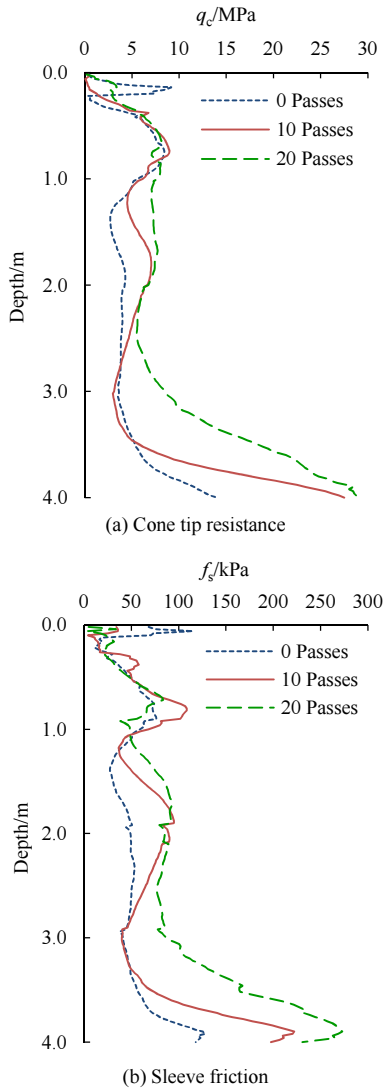

Fig.2　Variation with number of roller passes of CPT parameters

to the surface disturbance caused by the RDC module[9]. For this reason，the near-surface CPT records (＜0.1 m) have been removed from the dataset. However，below this depth (0.1 m onwards)，cone tip resistance is expected to increase with increasing number of roller passes，with a steady decrease down to the depth of influence，which is dependent on the subsurface material. It has been demonstrated by several researchers that RDC influences the ground to depths of 3 m and beyond depending on the soil type and ground conditions[5, 15, 17]. Hence，CPT measurements are considered to a depth of 4 m for each of the RDC project sites considered. Although the CPT readings from the RDC projects are available at 20 mm depth intervals，the values are averaged over 0.2 m depth intervals for each CPT sounding when incorporated in the ANN modeling in order to obtain a compromise between model parsimony and predictive accuracy. Figure 3 shows an example of this arithmetic averaging process with respect to cone tip resistance and sleeve friction.

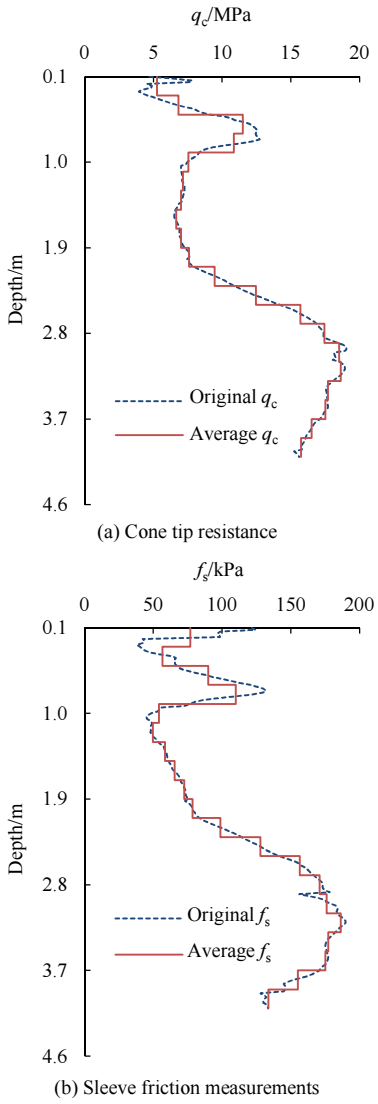

Fig.3　Example arithmetic average plots

3　Artificial neural networks (ANNs)

AI techniques，especially ANNs，have shown much better success in modelling complex problems than traditional approaches，due to their superior predictive ability. ANNs are one of the data-driven techniques that do not require a priori knowledge of the relationships between variables[18]. In spite of that，they utilize data to approximate both the optimal model structure as well as the unknown model parameters[19]. Thus，ANNs are well suited for

modeling complex problems，where non-linear patterns among the variables exist with undetermined relationships[20]. In contrast，most of the conventional statistical methods are model driven and often require the structure of the model to be established prior to parameter estimation[21]. Another advantage that ANNs possess over traditional statistical modeling，is their flexibility of implementation. A simple modification to the transfer function or the number of nodes in a hidden layer can greatly affect the ANN model′s complexity[21-22]. Additionally，a number of research studies have shown that ANNs overcome these limitations and outperform traditional methods，e. g. Y. M. Najjar，et al.[23-28].

In this study，CPT-based ANNs are developed for the prediction of the effectiveness of RDC. ANN modeling is carried out using the PC-based software，NEUFRAME version 4.0[29]. The process adopted in the ANN model development is well established in the literature[30] and involves the determination of model input (s)/output (s)，data division，selection of model architecture，optimization of network structure，model validation and performance evaluation.

Prior to model development，the database is divided into two subsets：

(1) Modeling dataset–This is used to train and validate the ANN models and consists of 1，755 records from 91 CPT soundings in total. This dataset is further divided into three subsets：training，testing and validation. Their statistics and applicability are discussed later in this paper.

(2) Verification dataset–Further verification of the developed ANN model is carried out by introducing a new unseen data set，which is not a part of the modeling stage in any capacity. The dataset comprises several CPT soundings randomly chosen from each of the RDC projects included in Table 1 and accounts for different numbers of roller passes. It is important to note that this particular dataset functions the same as the validation subset，but differs in that it contains the entire data record of each CPT sounding over the full depth (from 0.1 m to 4 m) and is not mixed with several other CPT soundings. A total of 222 records are used in the verification dataset taken from 12 CPT soundings.

In the present study，appropriate model inputs and outputs are defined based on the prior knowledge of the fundamental factors that influence ground density improvement by means of soil compaction. It is understood that the degree of soil compaction depends upon key factors including：the inherent physical properties of the soil，such as initial density，moisture content，soil type；and the amount of energy imparted to the ground. Therefore，4 parameters，the depth of measurement (D)，cone tip resistance (q_{ci}) and sleeve friction (f_{si}) prior to compaction，and the number of roller passes (P)，are selected as potential input variables for the ANN models. In order to predict the level of ground improvement，the models include a single output variable，the cone tip resistance after compaction (q_{cf}). The inclusion of sleeve friction，together with cone tip resistance，provides an indirect and useful representation of soil type in the ANN models through the friction ratio. The number of roller passes effectively expresses the amount of energy imparted to the soil，as the ANN model is unique to a specific RDC module；in this case the 4-sided，8 tonne impact roller. The statistics of model variables are graphically represented in Figure 4 and summarized in Table 2. It is worth noting that several other factors that affect the degree of soil compaction are not

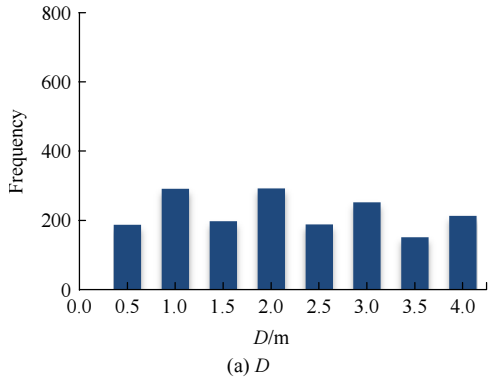

(a) D

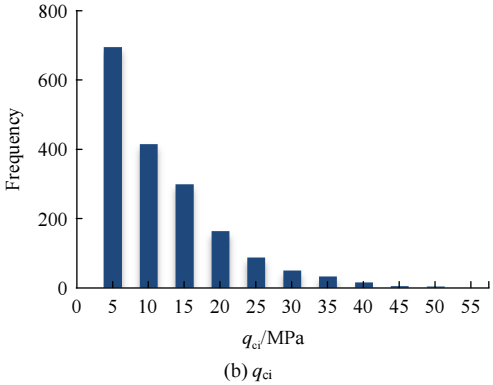

(b) q_{ci}

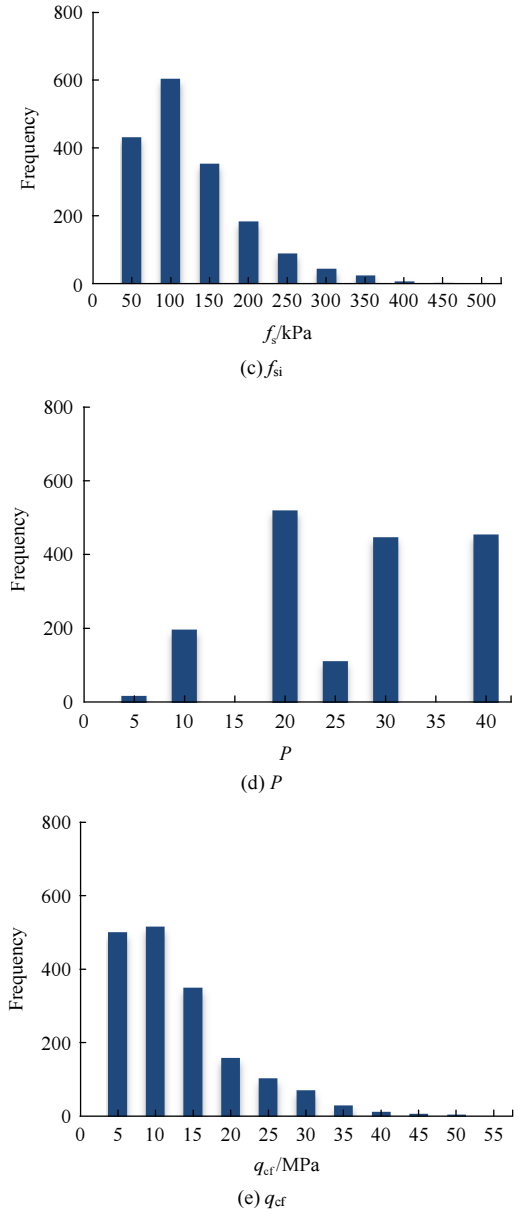

Fig.4　Histograms of the data used in the ANN model development

included in the models as direct input variables. Especially，the soil moisture content is not included as a direct measure due to the fact that such measurements were unavailable，as moisture content is not routinely measured，particularly in the case of cone penetration testing. However，it is apparent that penetration test results，including those from the CPT，are dependent upon the moisture content of the soil at the time of testing，and thus，soil moisture is indirectly incorporated in the selected model input variables.

Since the widely adopted cross validation technique[31] is used as the stopping criterion in the ANN model development，it requires the dataset to be divided into three subsets：training，testing and validation，as mentioned above. The training set is used to train and calibrate the model and it is with this data subset that the model′s connection weights are optimized. While the training progresses，model performance is assessed periodically with respect to the testing set. When the testing error begins to increase，even though the error obtained using the training set might continue to decrease，training is terminated to avoid overfitting and hence preserve its generalization ability. After model calibration，the validation data are used to validate the performance of the model using data unseen during model development. However，as described in the literature，e. g. A. S. Tokar，et al.[32-33]，the method used to divide the data into their subsets may adversely affect ANN model performance and thus in this study data division is carried out using self-organizing maps (SOMs)[34]. The SOM method is beneficial since it involves dividing the dataset in such a way that the subsets are statistically consistent and effectively represent the same population. The statistical properties considered in this study include the mean，standard deviation，minimum，maximum and range. ANNs are considered as an interpolation technique and models are expected to perform well when they do not extrapolate beyond the set limits of the training set[35-36]. Therefore，it is essential during data division to ensure that the training set contains all the possible patterns included in the dataset so that the final ANN model is as general

Table 2　Statistical properties of the data used in the ANN model development

Value types	Depth，D/m	Cone tip resistance prior to compaction，q_{ci}/MPa	Sleeve friction prior to compaction，f_{si}/kPa	No. of Roller Passes，P	Cone tip resistance after compaction，q_{cf}/MPa
Minimum	0.20	0.19	1.67	5.00	0.17
Maximum	4.00	50.65	473.86	40.00	50.36
Mean	1.98	9.34	102.78	26.69	10.44
Standard deviation	1.12	8.16	71.37	9.97	8.29

as possible. As such，it has been ensured that the maximum and minimum of each variable are included in the training dataset，which is ultimately employed for ANN model calibration. Moreover，with the aim of incorporating as many data patterns as possible within the training set，the data are divided in such a way that the training set contains 80% of the data and the remaining 20% are used for validation purposes. As such，a higher percentage of the total data is used in the training set to ensure that the model calibrated to as many data patterns as possible. However，the training set is further divided into two subsets；80% for training and 20% for testing. However，when using the SOM method there is no absolute rule when selecting the most favorable map size and，for that reason，several map sizes (e.g. 5×5，10×10) are examined and the map size which ensures the maximum number of clusters is considered to be optimal. Additionally，the datasets of each RDC project mentioned in Table 1 are individually subjected to SOM data division，rather than introducing the entire dataset into a single SOM. This ensures an even distribution of variables that represent the site-specific characteristics among the three subsets，and especially the training set，which will incorporate as many data patterns as possible. The selected optimal map sizes for the Port Botany and Potts Hill projects are 20×20 and 10×10，respectively，while 5×5 is optimal for the Outer Harbor，Banksmeadow and Cairns projects. Thereafter，the individually divided datasets are combined to form the three major subsets：training，testing and validation，and their statistics are shown in Table 3.

Table 3 ANN input-output summary statistics for the training，testing and validation data

Statistical parameters	Value types	Model variables				
		D/m	q_{ci}/MPa	f_{ci}/kPa	P	q_{cf}/MPa
Training	Mean	1.95	9.33	103.36	26.59	10.42
Testing		2.03	9.32	99.23	27.21	10.50
Validation		2.03	9.39	103.54	26.62	10.43
Training	Standard Deviation	1.11	8.23	71.76	9.94	8.30
Testing		1.14	8.37	71.29	9.64	8.66
Validation		1.14	7.83	70.37	10.30	8.03
Training	Minimum	0.20	0.19	1.67	5.00	0.17
Testing		0.20	0.30	8.70	5.00	0.29
Validation		0.20	0.32	7.08	5.00	0.39
Training	Maximum	4.00	50.65	473.86	40.00	50.36
Testing		4.00	47.39	441.04	40.00	45.12
Validation		4.00	47.94	470.29	40.00	46.20
Training	Range	3.80	50.46	472.19	35.00	50.19
Testing		3.80	47.09	432.34	35.00	44.83
Validation		3.80	47.63	463.21	35.00	45.81

Once the available data are divided into the three subsets，data pre-processing is carried out using the min-max normalization method. In data normalization，all model variables are scaled into a single range that is commensurate with the limits of the activation function used in the output layer[36]. This can expedite the model training rate and ensures that all the variables receive equal attention during the model training phase. For the ANN modelling undertaken in the present work，the logistic transfer function is used in the output layer and therefore the model variables are scaled between 0.1 and 0.9. Following the model calibration phase，it is necessary to de-normalize the network output by reverse scaling. In this work，multi-layer perceptron (MLP) models are developed with the use of the error back-propagation method. The feed forward type MLP is the most common network architecture used for prediction and forecasting applications[30] whereas，the error back-propagation method[37] is by far the most widely used algorithm for optimizing feed forward ANNs. A comprehensive description of the MLPs trained with the error back-propagation algorithm is beyond the scope of the paper but is well documented in the literature[38].

The selected MLP network architecture is comprised of three layers：the input layer，one hidden layer and the output layer. It has been demonstrated that one hidden layer can approximate any continuous function by providing a sufficient number of connection weights[39-40]. The number of nodes in the input and output layers represent the number of model inputs and outputs and thus the models consist of 4 nodes in the input layer：depth (D)，cone tip resistance (q_{ci}) and sleeve friction (f_{si}) prior to compaction and the number of RDC module passes (P). Since the models have a single output variable，i.e. cone tip resistance at depth (D) after the P module passes (q_{cf})，the output

layer consists of a single output node. Optimization of the number of hidden nodes is a crucial aspect of ANN model development and it is essential to achieve a structure that is neither too complex nor too simple but adequately captures the nuances contained in the training data. Therefore，to identify the optimal network architecture/topology a stepwise trial-and-error procedure is used，as is usual practice in ANN model development[30]. On this regard，several ANN models are trained，starting from the smallest possible network involving a single hidden node and successively increasing the number of hidden nodes to a maximum of 9. As suggested by M. Caudill[41]，*2I+1* is the upper limit of hidden nodes for a network to map any continuous function，with *I* being the number of input nodes，and accordingly 9 nodes are considered to be the maximum number of hidden nodes required for the models.

In order to obtain the optimal model，ANN parameters，such as learning rate，momentum and transfer function，are sequentially varied. ANN models are initially trained with the default software parameters (i.e. learning rate = 0.2，momentum term = 0.8 and the sigmoidal transfer function) are used for both the hidden and output layers. After determining the best topology，the network with the optimal number of hidden nodes is subjected to different combinations of learning rates and momentum terms. In addition，as the backpropagation algorithm is based on the steepest descent method，the obtained network results may be sensitive to the initial weight conditions[22]. Therefore，the selected ANN model is retrained several times after randomizing the initial weight allocations to ensure that model training does not cease at sub-optimal levels.

Upon the completion of ANN model calibration，the networks undergo model validation using the validation dataset. As mentioned earlier，this dataset is not used in the training process in any capacity and therefore，it is able to provide a rigorous assessment of the network′s predictive and generalization ability. The criteria used to evaluate the performance of the trained network include the root mean square error (*RMSE*)，mean absolute error (*MAE*) and coefficient of correlation (*R*). The prediction accuracy of a well-trained ANN model is represented by the smaller error values and an *R* value close to unity[42].

4　Results of ANN model optimization

The performance statistics of the developed models in terms of *RMSE*，*MAE* and *R* value are summarized in Table 4，where the model architecture，i.e. the number of hidden nodes，is varied. These performance measures are compared in order to select the optimum model topology which yields the best predictions.

As can be observed，good consistency is obtained with respect to the *RMSE*，*MAE* and *R* values among the three data sets：training，testing and validation. This implies that the model performance with respect to each of these three subsets is very similar，which in turn，indicates the given subsets represent the same population and that the SOM method for data division is effective. In order to select the optimal ANN model，as mentioned

Table 4　Performance results of ANN models with different numbers of hidden nodes

Hidden nodes	Training set			Testing set			Validation set		
	R	*RMSE*/MPa	*MAE*/MPa	*R*	*RMSE*/MPa	*MAE*/MPa	*R*	*RMSE*/MPa	*MAE*/MPa
1	0.844	4.59	3.11	0.860	4.61	3.11	0.850	4.38	3.07
2	0.861	4.27	2.87	0.860	4.48	2.99	0.859	4.14	2.82
3	0.861	4.26	2.87	0.861	4.45	2.98	0.859	4.13	2.82
4	**0.866**	**4.19**	**2.89**	**0.867**	**4.33**	**3.03**	**0.860**	**4.16**	**2.93**
5	0.872	4.13	2.89	0.868	4.34	3.09	0.853	4.29	3.06
6	0.872	4.14	2.90	0.869	4.33	3.07	0.853	4.29	3.07
7	0.865	4.21	2.91	0.866	4.35	3.04	0.860	4.17	2.94
8	0.866	4.17	2.85	0.867	4.32	2.97	0.860	4.13	2.87
9	0.862	4.23	2.84	0.863	4.41	2.95	0.859	4.12	2.79

previously，a compromise between predictive accuracy and model parsimony is sought. As such，when it is compared the performance statistics，the network with 4 hidden nodes，as shown in bold in Table 4，is deemed to have a strong correlation coefficient，i.e. $R>0.8$[42] and comparatively low prediction errors，i.e. *RMSE* = 4.16 MPa and *MAE* = 2.93 MPa with respect to the validation set data. Moreover，it can be observed that these performance statistics are consistent with the training and testing set data. However，at the same time，it is also apparent that the networks with a higher number of hidden layer nodes，for instance 7 and 8 hidden node networks，exhibit a slightly superior performance in terms of *R*，*RMSE* and *MAE* compared to those of the 4 hidden node network. Nevertheless，from a model parsimony perspective，the network with 4 hidden nodes is preferred. As a consequence，the model with 4 hidden nodes，as shown in bold in Table 4，is selected to be optimal. However，additionally，the multiple hidden layer (i.e. 2 and 3 hidden layers) models are also investigated but，a significant improvement in model performance over the selected optimal single layer model is not experienced. Therefore，in the interest of selecting a more parsimonious model，a single hidden layer，4 hidden node network is considered to be optimal，which also facilitates the development of a tractable and useable form of the ANN model，as will be discussed later. In order to refine further the model with 4 hidden layer nodes，the learning rate and the momentum terms are varied，as summarized in Table 5. From this analysis，it is observed that the model with a learning rate of 0.2 and momentum of 0.8 performs best.

Table 5 Effect of varying momentum terms and learning rates on the optimum model

Learning rate	Momentum term	Training set			Testing set			Validation set		
		R	*RMSE*/MPa	*MAE*/MPa	*R*	*RMSE*/MPa	*MAE*/MPa	*R*	*RMSE*/MPa	*MAE*/MPa
0.2	0.1	0.861	4.22	2.88	0.862	4.39	2.99	0.860	4.10	2.85
0.2	0.2	0.861	4.22	2.90	0.862	4.39	3.01	0.860	4.11	2.87
0.2	0.4	0.862	4.21	2.88	0.862	4.39	3.00	0.860	4.11	2.87
0.2	0.5	0.862	4.26	2.86	0.861	4.47	2.98	0.859	4.13	2.82
0.2	0.6	0.862	4.20	2.85	0.863	4.37	2.98	0.861	4.10	2.84
0.2	0.7	0.862	4.20	2.85	0.861	4.39	2.99	0.858	4.12	2.84
0.2	**0.8**	**0.866**	**4.19**	**2.89**	**0.867**	**4.33**	**3.03**	**0.860**	**4.16**	**2.93**
0.2	0.9	0.868	4.26	3.04	0.868	4.40	3.20	0.860	4.28	3.13
0.05	0.6	0.860	4.23	2.88	0.861	4.40	2.99	0.860	4.10	2.85
0.1	0.6	0.865	4.17	2.84	0.865	4.35	2.98	0.861	4.11	2.85
0.3	0.6	0.871	4.13	2.79	0.866	4.39	2.96	0.858	4.16	2.83
0.4	0.6	0.864	4.18	2.84	0.865	4.35	2.97	0.861	4.10	2.83
0.5	0.6	0.871	4.07	2.76	0.865	4.35	2.98	0.856	4.14	2.87
0.6	0.6	0.873	4.14	2.79	0.864	4.48	2.98	0.855	4.24	2.87
0.7	0.6	0.872	4.50	3.11	0.866	4.80	3.28	0.852	4.59	3.23
0.8	0.6	0.873	4.59	3.53	0.865	4.79	3.74	0.854	4.78	3.78
0.05	0.8	0.865	4.17	2.84	0.865	4.34	2.98	0.861	4.11	2.84
0.1	0.8	0.862	4.21	2.87	0.862	4.39	2.99	0.860	4.10	2.85
0.3	0.8	0.867	4.35	2.92	0.866	4.57	3.04	0.861	4.27	2.92
0.4	0.8	0.870	5.30	4.26	0.864	5.38	4.44	0.849	5.49	4.54
0.5	0.8	0.873	4.29	3.13	0.865	4.52	3.34	0.855	4.45	3.35
0.6	0.8	0.870	5.54	4.47	0.870	5.54	4.59	0.854	5.76	4.85
0.7	0.8	0.874	4.05	2.73	0.864	4.38	2.91	0.856	4.16	2.81
0.8	0.8	0.875	4.28	3.12	0.868	4.49	3.32	0.858	4.43	3.33

Figure 5 presents a plot of predicted and measured cone tip resistance after compaction (q_{cf}) with respect to the data in the testing and validation sets，in which the solid lines represent the linear trend line fitted to the predicted values and the dotted line indicates perfect prediction. It can be clearly seen that there is minimal scatter，the solid and dotted lines are in relatively close agreement，and hence the model performs well.

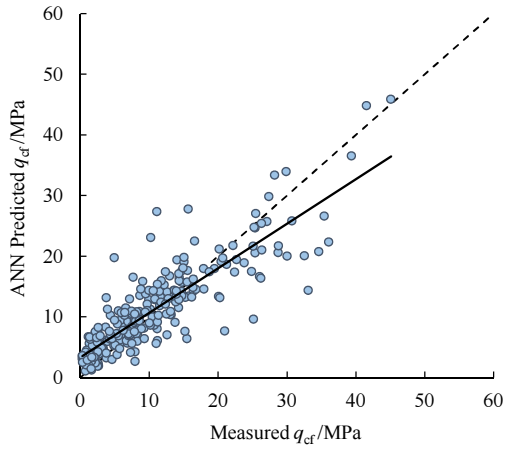

(a) Testing set data

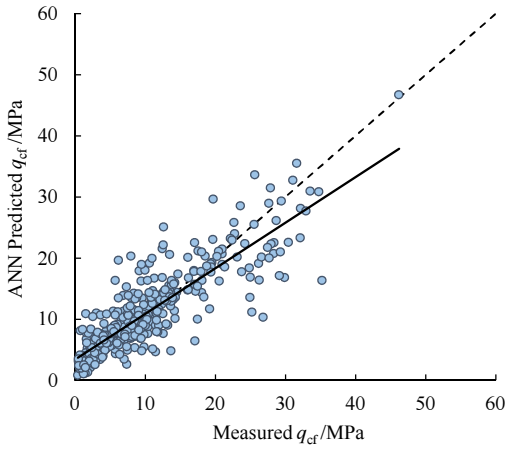

(b) Validation set data

Fig.5　Actual versus predicted q_{cf} for the optimum ANN model with respect to

As a further measure，the histogram of the optimal ANN model predictions versus the measured data with respect to the validation data set is shown in Figure 6. The *x*-axis presents the prediction error (PE) of the validation set，which is the ratio of model predicted q_{cf} to the measured q_{cf}，while the *y*-axis expresses the corresponding frequencies. As such，the solid line represents the distribution of PE，with ideal performance indicated by a ratio of unity，as shown on the figure by the dashed line. It can be clearly seen，with respect to the validation set data，that the PE distribution produces relatively high frequencies around unity. Hence，it is evident that the model predictions are in good agreement with the measured data.

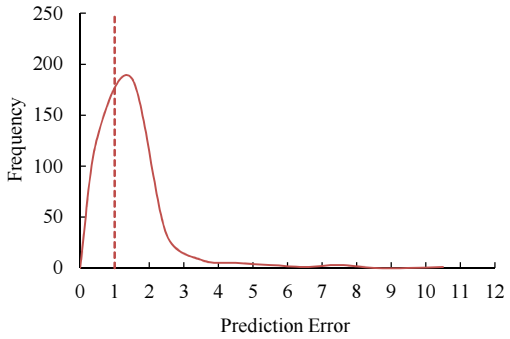

Fig.6　The distribution of the prediction error in the validation set data

5　Further verification of selected optimum ANN model

The capabilities of the optimal ANN model are further evaluated by introducing a series of unseen complete CPTs to the model. Details of this dataset were discussed earlier and the performance of the model with respect to these additional CPTs is summarized in Table 6 and Figure 7. As is evident，the model performs very favorably.

Table 6　Model performance on the verification data set

CPT location	*R*	*RMSE*/MPa	*MAE*/MPa
Port Botany - 30	0.955	3.63	3.39
Port Botany - 11	0.840	3.65	2.86
Port Botany - 45	0.971	6.06	5.30
Port Botany - 35	0.723	3.75	2.51
Potts Hill - 37/44	0.422	3.15	2.12
Potts Hill - 27/54	0.436	2.23	1.93
Potts Hill - 24/57	0.530	2.88	2.17
Outer Harbor - EFC 5	0.838	3.15	2.84
Banksmeadow - C3	0.141	2.49	1.90
Cairns-CPT 2	0.613	4.26	2.95
Cairns-CPT 5	0.794	2.83	2.31
Cairns-CPT 8	0.943	2.55	2.27

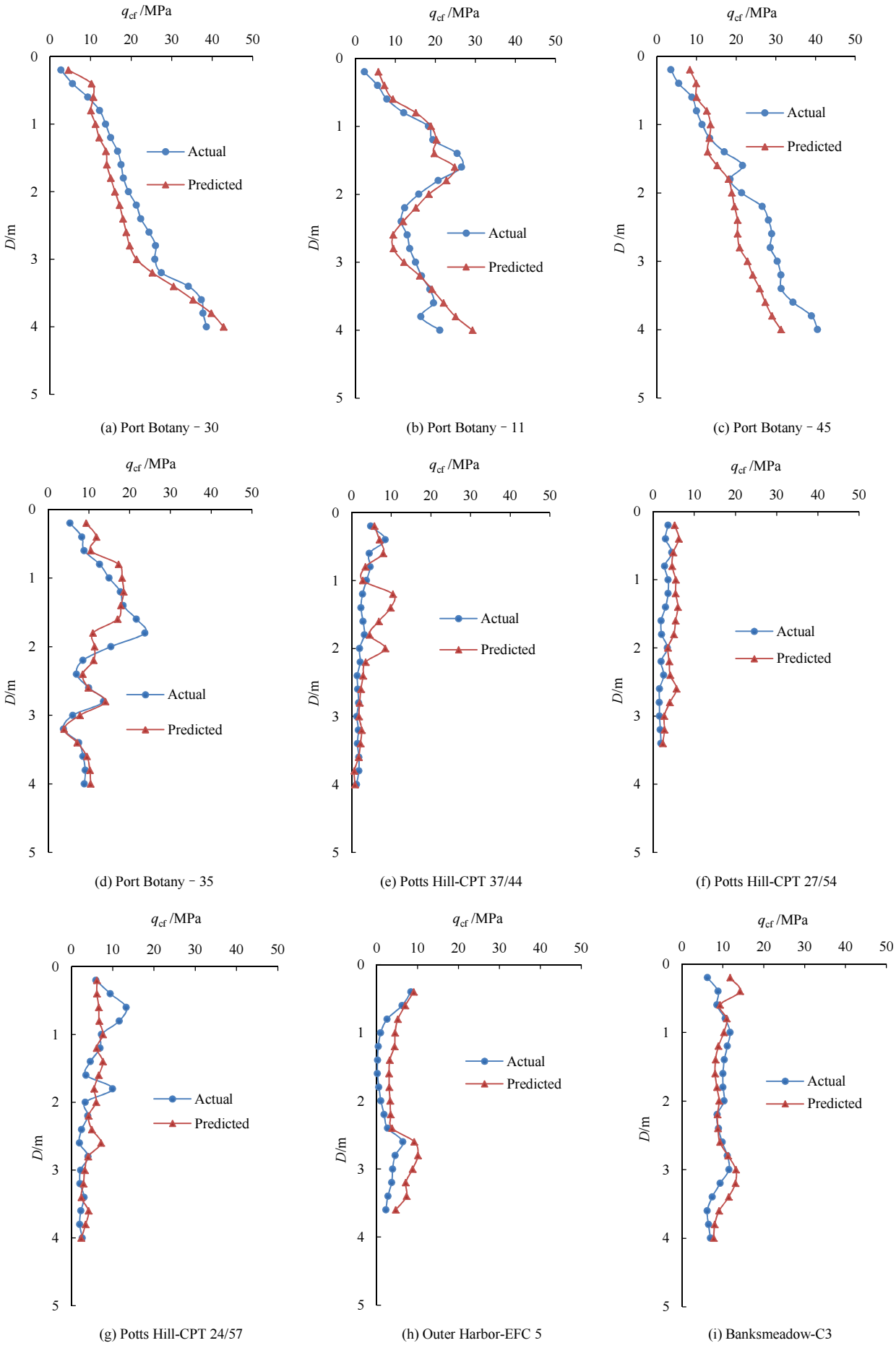

(a) Port Botany－30　(b) Port Botany－11　(c) Port Botany－45

(d) Port Botany－35　(e) Potts Hill-CPT 37/44　(f) Potts Hill-CPT 27/54

(g) Potts Hill-CPT 24/57　(h) Outer Harbor-EFC 5　(i) Banksmeadow-C3

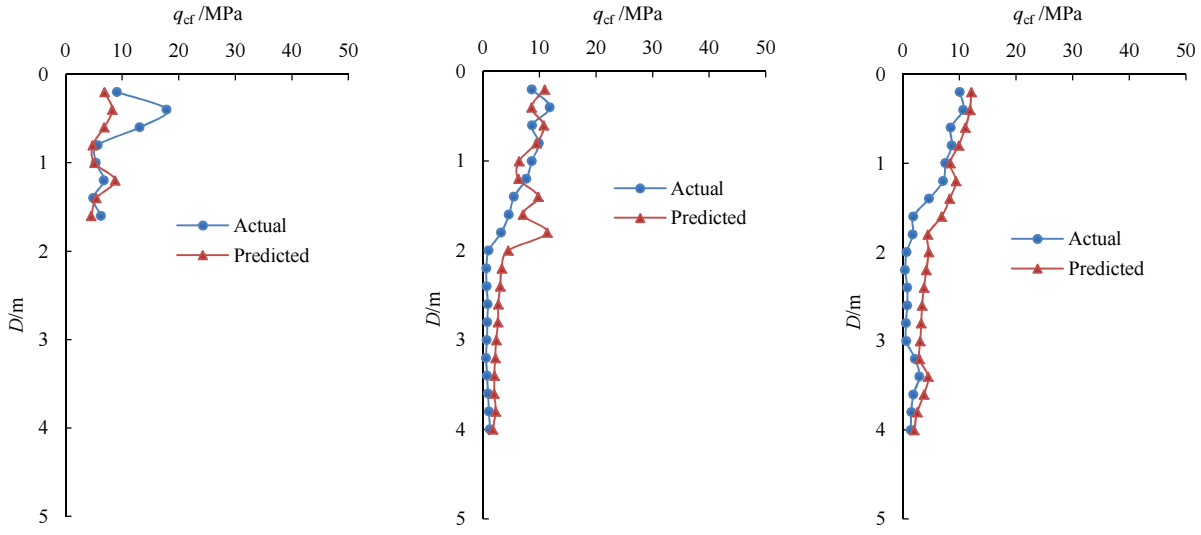

(j) Cairns-CPT 2　　(k) Cairns-CPT 5　　(l) Cairns-CPT 8

Fig.7　Plots of actual and model predicted CPT results

6　Robustness of the optimum ANN model

Finally，the validity and the accuracy of the optimal model are tested by examining how well the model predicts outputs that are consistent with the underlying physical behavior of the system. Therefore，to assess the generalization ability and the robustness of the selected optimal ANN model，a parametric study is carried out as recommended by M. A. Shahin et al.[43]. This involves investigating the response of the model output using a synthetic input data set，where the input variables are varied one at a time，while all other input variables remain at a pre-specified value. For this study，the output，q_{cf}，is examined while the input variables are varied in turn as follows：q_{ci} = 2，5，8，15，20 MPa，f_{si} = 50，100，150，200 kPa and P = 10，20，30，40. However，as mentioned earlier，ANNs perform best when they are used to interpolate[35]. Thus，the generated，hypothetical input variables are specified so that they lie within the ranges of the data used in the ANN model development. The resulting model predictions are presented in Figures 8 – 11.

It is observed that the model predictions from the

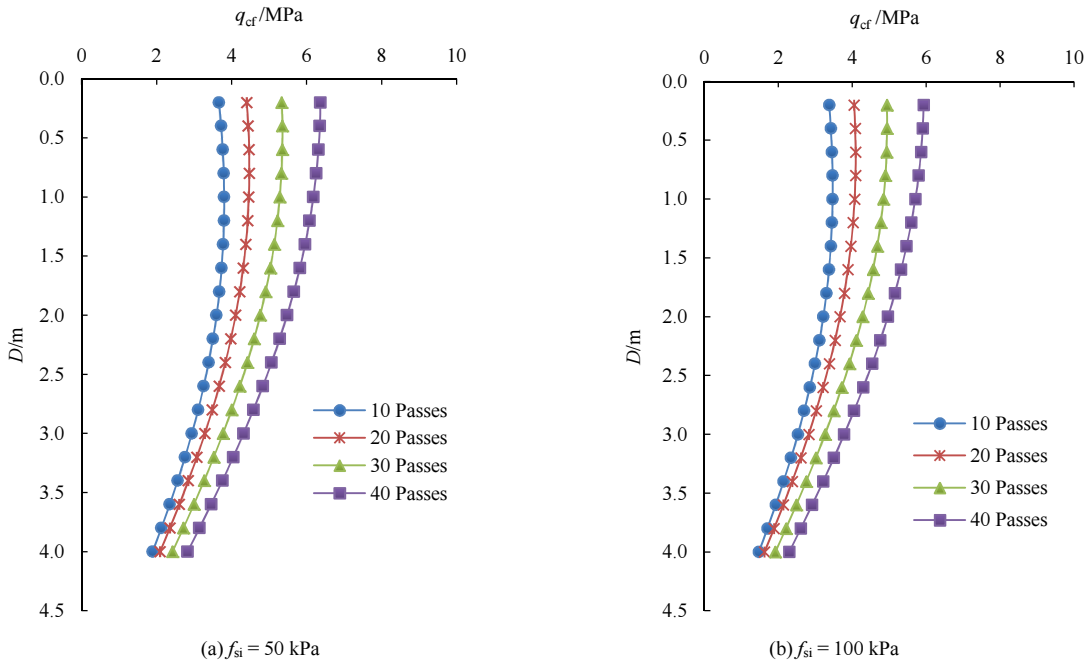

(a) f_{si} = 50 kPa　　(b) f_{si} = 100 kPa

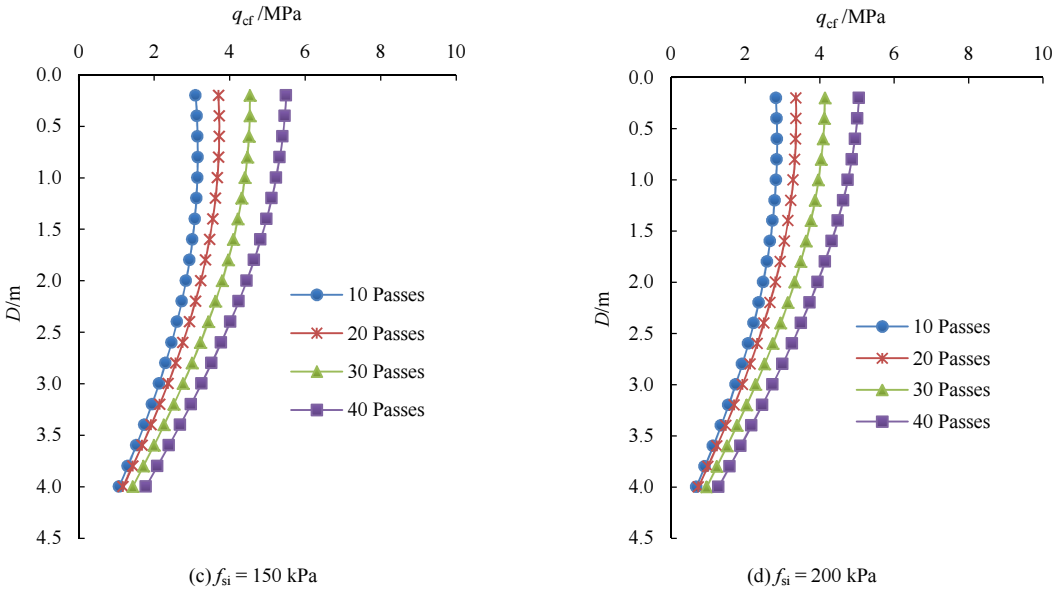

(c) f_{si} = 150 kPa　　(d) f_{si} = 200 kPa

Fig.8　Variation of q_{cf} with different number of roller passes at q_{ci} = 2 MPa

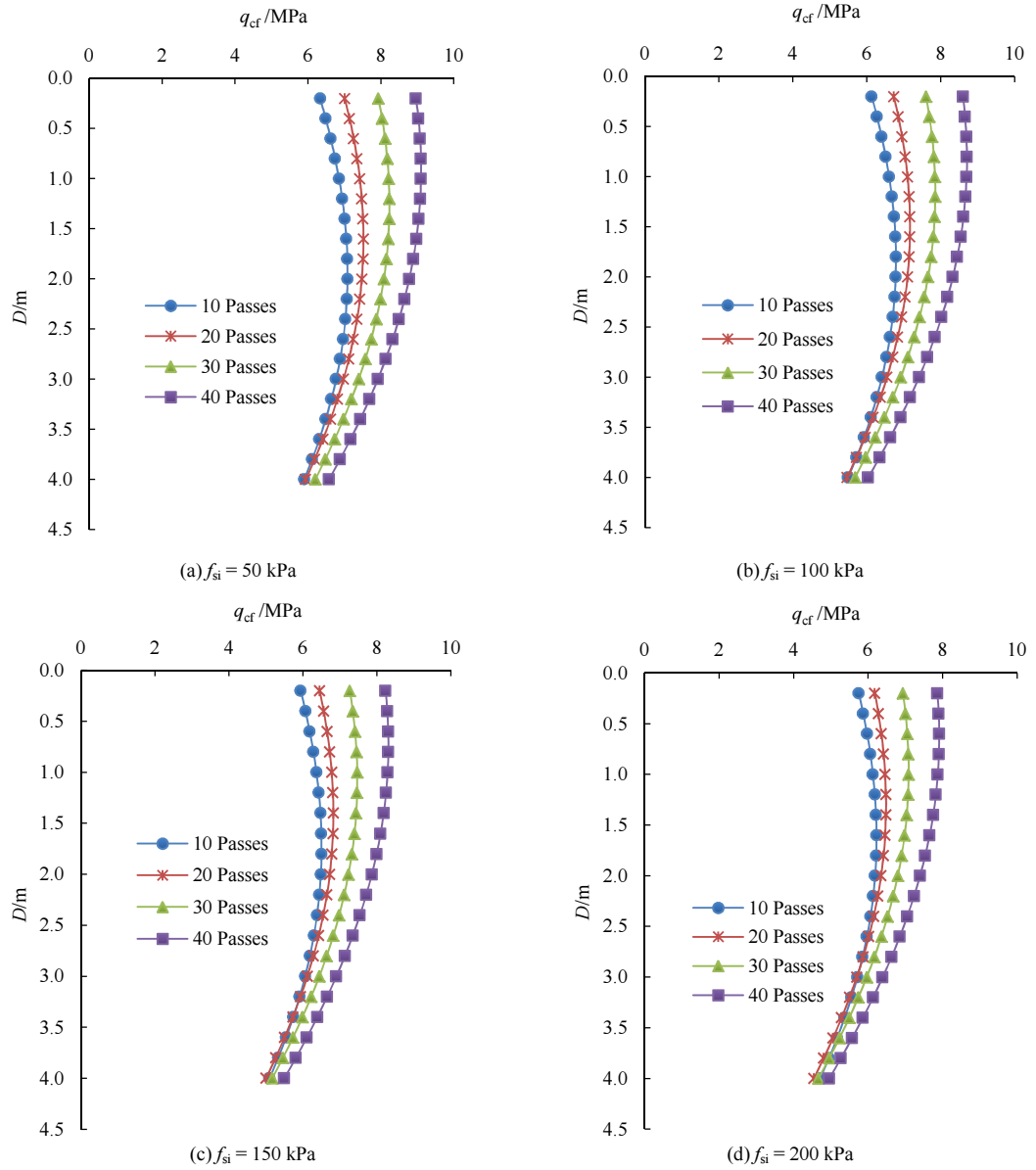

(a) f_{si} = 50 kPa　　(b) f_{si} = 100 kPa

(c) f_{si} = 150 kPa　　(d) f_{si} = 200 kPa

Fig.9　Variation of q_{cf} with different number of roller passes at q_{ci} = 5 MPa

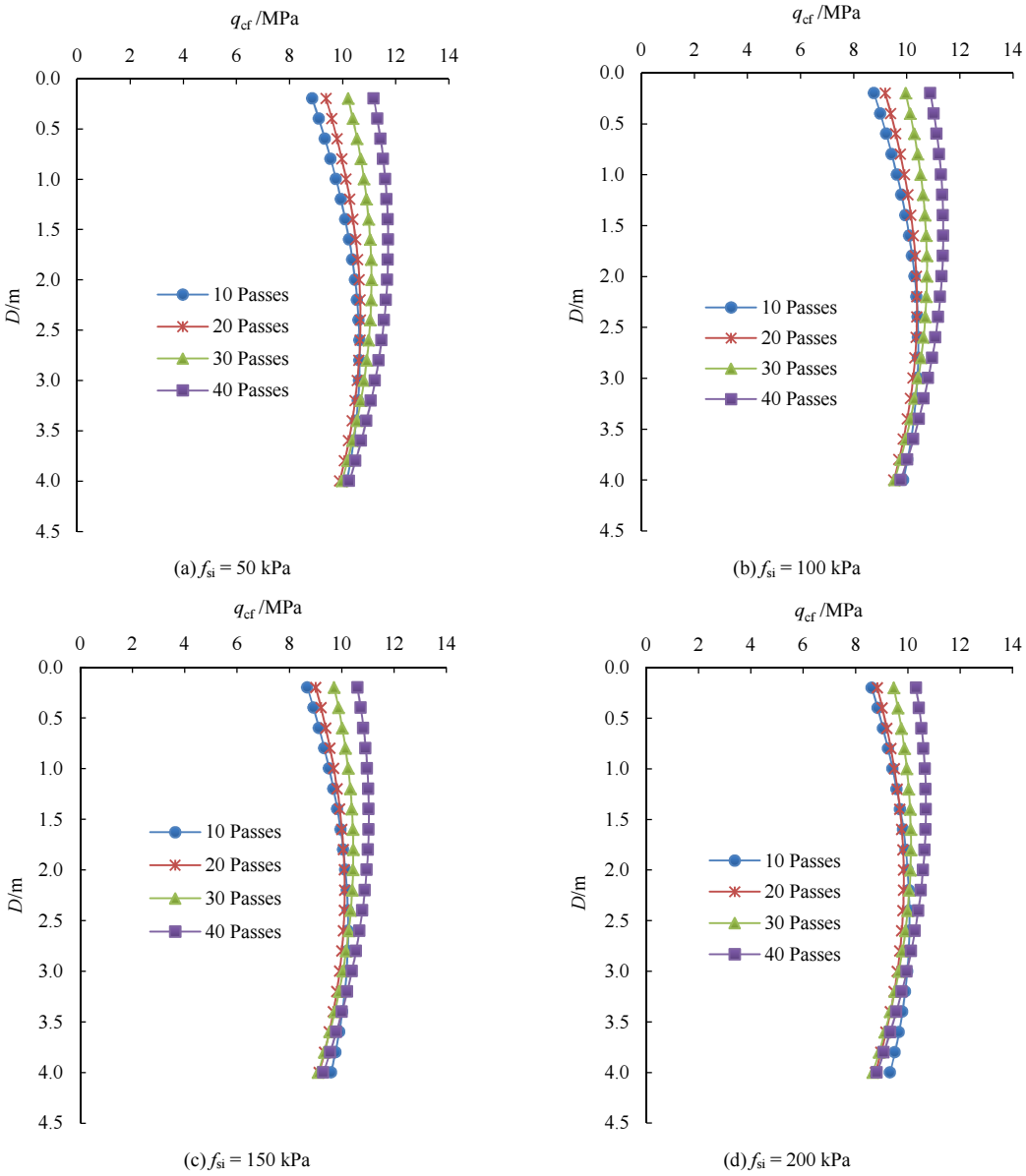

Fig.10　Variation of q_{cf} with different number of roller passes at q_{ci} = 8 MPa

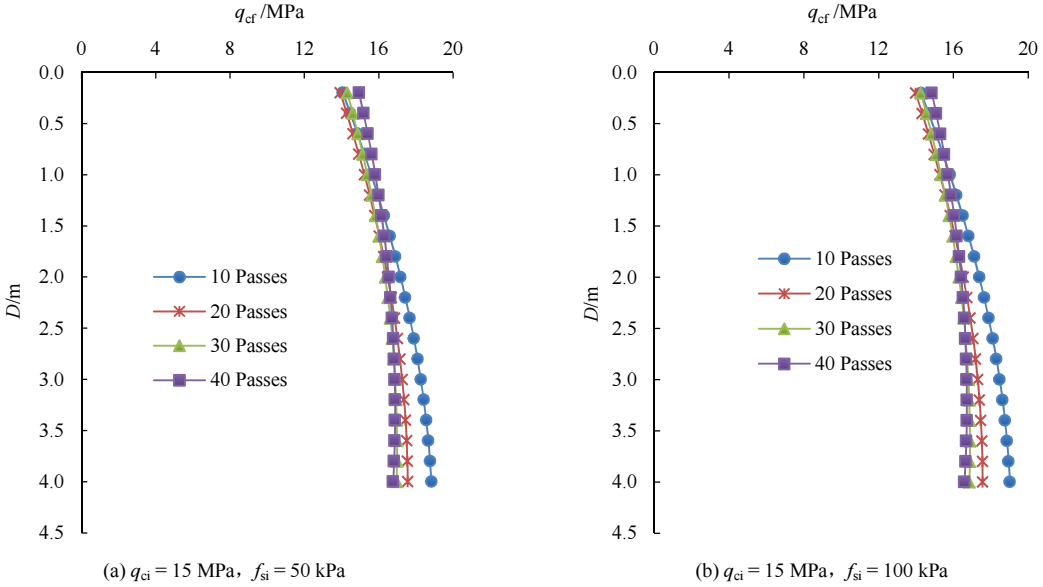

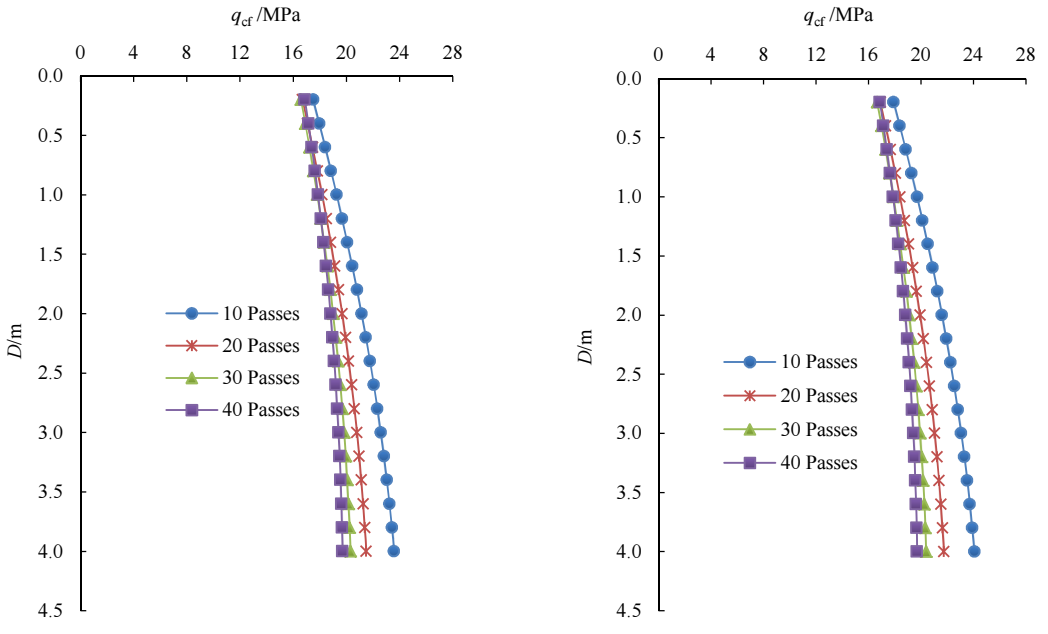

Fig. 11. Variation of q_{cf} with different number of roller passes

parametric study are in a good agreement with the expected behavior of RDC compaction. For instance，as illustrated in Figure 8(a)，there is a consistent increase in q_{cf} as the number of roller passes，P，increase from 10 to 40，while q_{ci} and f_{si} remain constant at 2 MPa and 50 kPa，respectively. These model predictions clearly demonstrate the improvement in strength resulting from the increasing number of roller passes at the same given location. Similarly，as shown in Figures 8(b) – (d)，increasing trends of q_{cf} with increasing P are also observed at different f_{si} values varying between 100 and 200 kPa while q_{ci} remains constant at 2 MPa. In addition，Figures 8 – 10 indicate that q_{cf} is less affected by f_{si}，resulting in only modest changes in the predicted q_{cf}. Nevertheless，it is evident from the parametric study that the distinct non-linear relationship between q_{cf} and P has been appropriately captured by the developed ANN model.

It is noted，from Figures 8 – 10，that the predictions of q_{cf} yield appropriate trends with increasing numbers of roller passes and depth. In contrast，however，Figure 11 displays less satisfactory predictions when the q_{ci} values are relatively large，e.g. 15 and 20 MPa，when the ground is initially quite dense. This may be attributed to the fact that the ANN model has been calibrated successfully mostly for lower values of q_{ci}. Figure 12 shows the histograms of both the q_{ci} and q_{cf} records included in the training dataset and which have been used in the model calibration. The dotted vertical lines indicate the mean values of q_{ci} and q_{cf} values in the training subset，which are 9.33 and 10.42，respectively. As indicated，the histograms for the q_c records contain a higher proportion in the lower range with respect to the mean values. Moreover，the data distributions are skewed to the left-hand side and exhibit sharp peaks rather than being normally distributed around the mean. Hence，as a result of this，it is likely that the model predictions are less satisfactory with regards to soil with high q_{ci} values because of the paucity of such data available from previous RDC projects. This is likely due to the

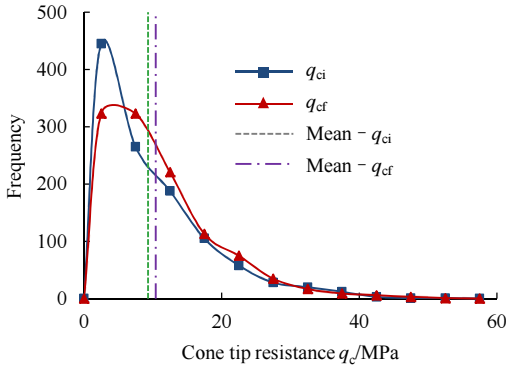

Fig.12　Data distribution of cone tip resistance values in training data set

fact that RDC is normally applied to ground which is initially loose and not dense. Hence，it is suggested that the optimal ANN model can be used with confidence when the q_{ci} values are below 10 MPa.

7　MLP-based Equation

Having finalized the optimal MLP model，in order to facilitate its adoption in practice，it is disseminated as a series of simplified equations. The optimal model structure is shown in Figure 13 and the associated weights and biases are presented in Table 7. These weights are utilized in the development of the equation resulting from the ANN model.

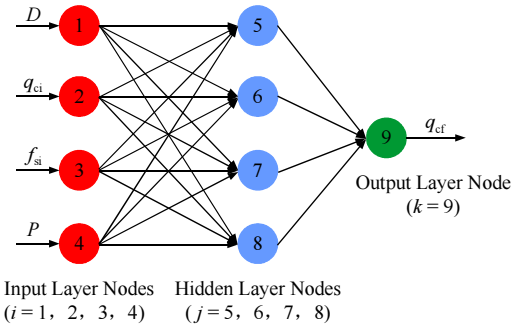

Fig.13　The structure of the optimum four hidden nodes network

The equation，which relates the input and output variables[44] can be written as follow：

$$O_{k=9} = f_{sig}\left\{\theta_k + \sum_{j=5}^{8}\left\{W_{kj} f_{sig}\left[\theta_j + \sum_{i=1}^{4}(W_{ji} I_i)\right]\right\}\right\} \quad (1)$$

Where，O_k is the single output variable，θ_k is the threshold value of the k^{th} output node in the output layer and W_{kj} is the connection weight between the j^{th} node in the hidden layer and the k^{th} node in the output layer. Similarly，θ_j is the threshold value of the j^{th} hidden node and W_{ji} is the connection weight between the i^{th} input node and the j^{th} hidden node. The parameter I_i is the i^{th} input variable and f_{sig} is the sigmoid transfer function.

Equation (1) can be simplified as follows：

$$O_{k=9} = \frac{1}{1+e^{-\left[\theta_k + \sum_{j=5}^{8}(W_{kj} T_j)\right]}} \quad (2)$$

and

$$T_{j=5,\ \cdots,8} = \frac{1}{1+e^{-\left[\theta_j + \sum_{i=1}^{4}(W_{ji} I_i)\right]}} \quad (3)$$

The input variables I_1，I_2，I_3 and I_4 represent the depth below the ground surface (m)，q_{ci} (MPa)，f_{si} (kPa) and the number of roller passes，P，respectively. However，it should be noted，as mentioned above，that the input variables are required to be scaled down prior to them being used in Equations (2) and (3). Therefore，the actual input variables ($I_{unscaled}$) are scaled between 0.1 and 0.9 using Equation (4) in accordance with the given extremes of the training dataset which has been shown in Table 3.

$$I_{scaled} = a + \frac{(I_{unscaled} - A)(b-a)}{(B-A)} \quad (4)$$

Where，A and B are the minimum and maximum values of the unscaled dataset，respectively. Similarly，the minimum and maximum values of the scaled dataset are denoted by a and b，which are equal to 0.1 and 0.9 in this study.

With reference to Figure 13 and according to the connection weights in Table 7，the mathematical equation for the optimal ANN model containing 4

Table 7　Weights and threshold levels of the optimum ANN model

Hidden nodes	Weight from node i in the input layer to node j in the hidden layer w_{ji}				Hidden layer threshold (θ_j)
	i =1	i =2	i =3	i =4	
j = 5	1.190	–8.585	0.754	–0.128	–1.200
j = 6	–1.677	–1.592	0.310	–1.300	0.224
j = 7	–0.709	–1.474	0.157	–0.369	–0.232
j = 8	0.123	3.546	1.211	–2.277	–3.149
Output nodes	**Weight from node j in the hidden layer to node k in the output layer w_{kj}**				**Output layer threshold (θ_k)**
	j = 5	j = 6	j = 7	j = 8	
k = 9	–6.172	–1.819	–0.916	3.820	–0.113

hidden nodes can be re-written as follows：

$$q_{cf} = \frac{62.738}{1+\exp(6.172T_5+1.819T_6+0.916T_7-3.82T_8+0.113)} - 6.104$$

And，

$$\left.\begin{aligned} T_5 &= [1+\exp(-0.251I_1+0.137I_2-0.002I_3+0.003I_4+1.889)]^{-1} \\ T_6 &= [1+\exp(0.354I_1+0.025I_2-0.001I_3+0.03I_4-0.023)]^{-1} \\ T_7 &= [1+\exp(0.15I_1+0.024I_2-0.000\,3I_3+0.008I_4+0.395)]^{-1} \\ T_8 &= [1+\exp(-0.026I_1-0.057I_2-0.002I_3+0.052I_4+2.647)]^{-1} \end{aligned}\right\} \quad (5)$$

8 Summary and conclusions

This paper presents a new and unique model to predict the performance of rolling dynamic compaction (RDC) based on the artificial intelligence technique known as artificial neural networks (ANNs). The model is developed using a database consisting of cone penetration test (CPT) results obtained from several ground improvement projects which employed the 4-sided，8 tonne“impact roller”. The model utilizes 4 input variables，including depth (m)，cone tip resistance prior to compaction (MPa)，sleeve friction prior to compaction (kPa) and the number of roller passes to obtain the cone tip resistance after compaction (MPa)，as the sole output.

The resulting optimal ANN model yields relatively accurate predictions with a coefficient of correlation (R) of 0.86 and a root mean square error ($RMSE$) of 4.16 MPa，when validated against a set of unseen data. The performance of the optimal ANN model has been further verified by introducing a series of complete and unseen CPT soundings. The resulting model predictions are in very good agreement with the actual CPT records. The robustness of the optimal model is further investigated by conducting a parametric study and it is observed that the predicted model outputs agree well with the underlying physical behavior of the system. It is concluded that the selected optimal network is robust and reliable for values of initial cone resistance (q_{ci}) less than or equal to 10 MPa. However，the model is not well calibrated for the higher values of q_{ci} due to the paucity of such data in the existing CPT database. However，the applicability and the accuracy of the developed models can be further enhanced by incorporating more data from additional RDC-related projects that may become available in the future. As such，it is desirable to include a dataset where the input parameters span a wider range than in the existing dataset. Nevertheless，in order to disseminate the optimal model and to facilitate its use in practice，it is expressed as a series of tractable equations which can be incorporated into a spreadsheet or calculated by hand. As with all ANN models，they perform best when interpolating within the data ranges used in the model′s development. These are given in the body of the paper. The model is intended to provide initial predictions for planning purposes and not to replace field trials，which will yield more accurate and site-specific conclusions.

Acknowledgements

This research was supported under Australian Research Council′s Discovery Projects funding scheme (project number DP120101761). The authors wish to acknowledge Mr. Stuart Bowes at Broons Hire (SA) Pty Ltd for his kind assistance and continuing support，especially in providing access to the in situ test results upon which the numerical models are based. The authors are also grateful to Mr. Brendan Scott for his contribution to this work.

References：

[1] HAUSMANN M R. Engineering principles of ground modification[J]. New York：McGraw-Hill，1990.

[2] PINARD M I. Innovative developments in compaction technology using high energy impact compactors[C]// 8th Australia New Zealand Conference on Geomechanics：Consolidating Knowledge. Hobart，Australia：Australian Geomechanics Society，1999.

[3] AVALLE D L. Use of the impact roller to reduce agricultural water loss[C]// 9th ANZ Conference on Geomechanics. Auckland，New Zealand：Citeseer，2004.

[4] PINARD M I，OOKEDITSE S. Evaluation of high energy impact compaction techniques for minimising construction water requirements in semi arid regions[C]// 14th Australian Road Research Board (ARRB) Conference. Canberra，Australia：ARRB Group Limited，1988.

[5] AVALLE D L，CARTER J P. Evaluating the improvement from impact

rolling on sand[C]// 6th International Conference on Ground Improvement Techniques. Coimbra，Portugal：[s. n.]，2005.

[6] CLEGG B，BERRANGÉ A R. The development and testing of an impact roller[J]. The Civil Engineer in South Africa，1971，13(3)：65－73.

[7] CLIFFORD J M. Impact rolling and construction techniques[C]// Australian Road Research Board Conference. Perth，Australia：[s. n.]，1976，8：21－29.

[8] CLIFFORD J M. The impact roller-problem solved[J]. The Civil Engineer in South Africa，1978，20(12)：321－324.

[9] AVALLE D L. Reducing haul road maintenance costs and improving Tyre wear through the use of impact rollers[C]// Mining for Tyres Conference. Perth，Australia：[s. n.]， 2006.

[10] AVALLE D L，YOUNG G. Trial programme and recent use of the impact roller in Sydney[C]// Earthworks Seminar， Australian Geomechanics Society. Adelaide，Australia：[s. n.]， 2004

[11] SCOTT B T，JAKSA M B. Mining applications and case studies of rolling dynamic compaction[C]// 11th Australia-New Zealand (ANZ) Conference on Geomechanics. Melbourne，Australia：[s. n.]，2012.

[12] ROBERTSON P K. Soil classification using the cone penetration test[J]. Canadian Geotechnical Journal，1990，27(1)：151－158.

[13] ASTM D5778－95 Standard test method for performing electronic friction cone and piezocone penetration testing of soils[S]. West Conshohocken：ASTM International，2000.

[14] LUNNE T，ROBERTSON P K，POWELL J J M. Cone penetration testing in geotechnical engineering practice[M]. New York，USA：Blackie Academic and Professional，1997.

[15] KELLY D B. Deep in-situ ground improvement using high energy impact compaction (Heic)[C]// Technology International Conference on Geological and Geotechnical Engineering. Melbourne，Australia：International Society for Rock Mechanics，2000.

[16] SCOTT B T，JAKSA M B. Evaluating rolling dynamic compaction of fill using CPT[C]// 3rd International Symposium on Cone Penetration Testing. Las Vegas，Nevada，USA：Omni Press，2014.

[17] JAKSA M B，SCOTT B T，MENTHA N L，et al. Quantifying the zone of influence of the impact roller[C]// International Symposium on Ground Improvement Brussels. Belgium：[s. n.]，2012， II：41－52.

[18] LACHTERMACHER G， FULLER J D. Backpropagation in hydrological time series forecasting[J]. Stochastic and Statistical Methods in Hydrology and Environmental Engineering，1994，10(3)：229－242.

[19] SHAHIN M A. Intelligent computing for modeling axial capacity of pile foundations[J]. Canadian Geotechnical Journal，2010，47(2)：230－243.

[20] MAIER H R，DANDY G C. The use of artificial neural networks for the prediction of water quality parameters[J]. Water Resources Research，1996，32(4)：1 013－1 022.

[21] SHAHIN M A，MAIER H R，JAKSA M B. Predicting the settlement of shallow foundations on cohesionless soils using back-propagation neural networks[M]. Adelaide，Australia：Department of Civil and Environmental Engineering，University of Adelaide，2000.

[22] MAIER H R，DANDY G C. Neural networks for the prediction and forecasting of water resources variables：a review of modelling issues and applications[J]. Environmental Modelling and Software，2000，15(1)：101－124.

[23] NAJJAR Y M，BASHEER I A，NAOUSS W A. On the identification of compaction characteristics by neuronets[J]. Computers and Geotechnics，1996，18(3)：167－187.

[24] GÜNAYDIN O. Estimation of soil compaction parameters by using statistical analyses and artificial neural networks[J]. Environmental Geology，2009，57(1)：203－215.

[25] POOYA NEJAD F，JAKSA M B，KAKHI M，et al. Prediction of pile settlement using artificial neural networks based on standard penetration test data[J]. Computers and Geotechnics，2009，36(7)：1 125－1 133.

[26] SULEWSKA M J. Neural modelling of compactibility characteristics of cohesionless soil[J]. Computer Assisted Mechanics and Engineering Sciences，2010，17(1)：27－40.

[27] CHOK Y H，JAKSA M B，KAGGWA W S，et al. Neural network prediction of the reliability of heterogeneous cohesive slopes[J]. International Journal for Numerical and Analytical Methods in Geomechanics，2016，40(11)：1 556－1 569.

[28] POOYA NEJAD F，JAKSA M B. Load-settlement behavior modeling of single piles using artificial neural networks and CPT data[J]. Computers and Geotechnics，2017，89：9－21.

[29] Neusciences. Neuframe version 4.0[M]. Southampton，Hampshire：Neusciences Corp.，2000.

[30] MAIER H R，JAIN A，DANDY G C，et al. Methods used for the development of neural networks for the prediction of water resource variables in river systems： current status and future directions[J]. Environmental Modelling and Software，2010，25(8)：891－909.

[31] STONE M. Cross-validatory choice and assessment of statistical predictions[J]. Journal of the Royal Statistical Society Series B-Statistical Methodology，1974，36(2)：111－147.

[32] TOKAR A S，JOHNSON P A. Rainfall-runoff modeling using artificial neural networks[J]. Journal of Hydrologic Engineering，1999，4(3)：232－239.

[33] SHAHIN M A，MAIER H R，JAKSA M B. Data division for developing neural networks applied to geotechnical engineering[J]. Journal of Computing in Civil Engineering，2004，18(2)：105－114.

[34] BOWDEN G J，MAIER H R，DANDY G C. Optimal division of data for neural network models in water resources applications[J]. Water Resources Research，2002，38(2)：2－11.

[35] FLOOD I，KARTAM N. Neural networks in civil engineering. I：principles and understanding[J]. Journal of Computing in Civil Engineering，1994，8(2)：131－148.

[36] MINNS A W，Hall M J. Artificial neural networks as rainfall-runoff models[J]. Hydrological Sciences Journal，1996，41(3)：399－417.

[37] RUMELHART D E，HINTON G E，WILLIAMS R J. Learning representations by backpropagating errors. cognitive modeling[M]. POLK T A，SEIFERT C M. London，UK：The MIT Press，1986：213－221.

[38] FAUSETT L V. Fundamentals of neural networks：architectures，algorithms，and applications[M]. New Jersey，USA：Prentice-Hall，Inc.，1994.

[39] CYBENKO，G. Approximation by superpositions of a sigmoidal function[J]. Mathematics of Control，Signals and Systems，1989，2(4)：303－314.

[40] HORNIK K，STINCHCOMBE M，WHITE H. Multilayer feedforward networks are universal approximators[J]. Neural Networks，1989，2(5)：359－366.

[41] CAUDILL M. Neural networks primer，part III[J]. AI Expert，1988，3(6)：53－59.

[42] SMITH M Neural networks for statistical modeling[M]. New York，USA：Thomson Learning，1993.

[43] SHAHIN M A，JAKSA，M B，MAIER H R. Neural network based stochastic design charts for settlement prediction[J]. Canadian Geotechnical Journal，2005，42(1)：110－120.

[44] DAS S K，SAMUI P，SABAT A. K. Application of artificial intelligence to maximum dry density and unconfined compressive strength of cement stabilized soil[J]. Geotechnical and Geological Engineering，2011，29(3)：329－342.